Radiative Emission Fraction of Pool Fires Burning Silicone Fluids

R. BUCH,** A. HAMINS,* K. KONISHI,† D. MATTINGLY,†† and T. KASHIWAGI

Building and Fire Research Laboratory, National Institute of Standards and Technology, Gaithersburg, MD 20899

The steady-state mass burning flux and the radiative flux profiles to the surroundings were measured for a series of burning silicone fluids and organic fuels in 0.1-m, 0.3-m, 0.6-m and 1-m pool burners. Short-chain silicone oligomers and aliphatic/aromatic hydrocarbons exhibited a strong dependence of the mass flux and the radiative fraction on pool size. The longer chain length silicone fluids and alcohols exhibited both markedly lower mass fluxes and radiative components of heat release and these parameters were virtually independent of pool size. Silica, a gas-phase combustion product of the silicone fluids, was observed to deposit into the vaporizing liquid pool, the yield increasing with silicone chain length. This necessitated correcting the measured apparent mass flux for the liquid volume displaced by the silica. The measured radiative power emitted from flames burning silicone oligomers and hydrocarbons was substantially larger than the power radiated by flames burning long-chain silicone fluids or alcohols. The mass gasification flux and the radiative fraction of the silicones fluids and the organic fuels were well correlated by the ratio of the heat of combustion to the heat of gasification of the fluids.

INTRODUCTION

Silicones encompass a wide variety of materials, for example, fluids, foams, sealants, resins, and elastomers. Currently, silicon-based materials are being evaluated as potential replacements for halogenated compounds as cleaning solvents, cable compounds, fire-retardant additives, and other applications. In addition to their unique surface, physical, and chemical properties, several products (e.g., industrial transformer fluid, fire-barrier foam, thermal ablatives) rely to a large extent on the unique fire properties of silicones. Most notably, silicones exhibit low heat-release rates regardless of pool size [1–3] and fire severity [4]. Lipowitz et al. proposed a model for the combustion of these materials [5, 6]. Previous studies [1–3] of the pool burning of silicone fluids have been limited in the number of fluids tested and have not measured the spatial distribution of radiative flux nor the global radiation properties under steady mass burning flux conditions, an important consideration for measurement accuracy. Unique to this study, the importance of silica ash deposition back to the burning pool and its influence on the apparent mass burning rate was quantified for a range of silicone fluids.

The fluids studied were octamethylcyclotetrasiloxane, $[(CH_3)_2SiO]_4$ and a series of trimethylsiloxy end-blocked polydimethylsiloxane (PDMS) fluids, $[(CH_3)_3Si\text{-}O[\text{-}Si(CH_3)_2\text{-}O]_n\text{-}Si(CH_3)_3]$, where n indicates the average chain length, that is, the number of siloxane units in the molecule. Commercial silicones are based on dimethyl substituents on silicon, hence the acronym PDMS. A convenient shorthand notation for PDMS molecules is: MD_nM where $M = (CH_3)_3SiO_{1/2}$, $D = (CH_3)_2SiO$, and n is the chain length. These fluids are typically referred to by their viscosity, which increases with the average chain length as shown in Table 1 [7]. For comparison, the properties of a number of organic compounds are also listed in Table 1. Other properties presented in Table 1 include the fluid boiling point (T_b), the heat of gasification (H_g), the net heat of combustion (H_c), and the ratio of the net heat of combustion to the heat of gasification (H_c/H_g), which is related to the diffusive transfer (B) number cited in the literature [8]. Table 1 shows that H_c/H_g has values similar to those of the organic fluids. The longer chain silicones, which consist of a distri-

* Corresponding author.

** Present address: Dow Corning Corp., 2200 W. Salzburg Rd., Auburn, MI, 48611; † Saitama Institute of Technology, Okabe, Japan 369-02; †† NIST summer intern.

0010-2180/97/$17.00
PII S0010-2180(96)00098-3

COMBUSTION AND FLAME 108: 118–126 (1997)

Published by Elsevier Science Inc.

bution of various chain length molecular species, are characterized by a very high T_b and do not exhibit a specific boiling point temperature. Thus, H_g in Table 1 represents an estimate for these compounds. A unique radiative gasification apparatus is currently being used at National Institute of Standards and Technology (NIST) to measure the global H_g for silicones accurately.

Insight into the burning behavior of PDMS is evident from the stoichiometry of complete combustion:

$$(CH_3)_3Si\text{-}O[\text{-}Si(CH_3)_2\text{-}O]_n\text{-}Si(CH_3)_3 \rightarrow +(12 + 4n)O_2 8 \rightarrow (2 + n)SiO_2 + (6 + 2n)CO_2 + (9 + 3n)H_2O \quad (1)$$

where, for example, the combustion of 1 mole of MD_1M leads to the formation of 3 moles of SiO_2, a fine, white particulate ash. Amorphous silica is a major combustion product and its deposition on the surface of a burning pool plays a significant role in the heat and mass transfer processes for these materials. Equation 1 indicates the combustion products emitted from PDMS fires include CO_2, H_2O, and SiO_2, which is a fully oxidized particulate. In a silicone fluid fire a portion of the silica (SiO_2) ash is carried away by the buoyant fire plume and a portion of the ash falls, returning to the pool. The ash is an important influence on the burning behavior of PDMS in terms of the intensity and spectral character of the radiative emission and because a portion of the ash falls back onto the fuel surface where it acts to absorb incident radiation and mediates the gasification process. The deposition of gas-phase silica on the pool surface is a major difference between fires burning hydrocarbon and silicone fluids. Furthermore, smoke yield from a burning organic fuel results from a competition between soot production (nucleation and growth) and soot oxidation. Silica ash, on the other hand, is a stable oxidized combus-

TABLE 1

Properties of Silicone and Organic Fluids[a]

Fluid viscosity (cS, 298 K) or organic	Fluid Description[b]	T_b (°C)	H_g[c] (J/g)	H_c[g] (kJ/g)	H_c/H_g	T_{pool}(°C) 10-cm burner	T_{pool}(°C) 30-cm burner
0.65	MM	100	349	33.8	97	—	—
1.0	MD_1M	153	401	30.9	77	—	—
1.5	MD_2M	194	457	28.8	63	130	—
2.3	D_4	176	416	24.8	60	145	—
2.0	MD_3M	230	505	28.0	55	—	—
5.0	MD_8M[d]	*	*	24.8	*	183	—
10	$MD_{15}M$[d]	*	≈ 3300	24.8	≈ 7.5	190	220
20	$MD_{28}M$[d]	*	≈ 3300	24.8	≈ 7.5	210	—
50	$MD_{58}M$[d]	≈ 370[e]	≈ 3300	24.8	≈ 7.5	242	330
Toluene	C_7H_8	110	526	40.5	77	—	—
Heptane	C_7H_{16}	98	499	44.6	89	78	—
Acetone	C_3H_6O	56	585	28.6	49	—	—
MMA[f]	$C_5H_8O_2$	100	503	25.6	51	—	—
Ethanol	C_2H_5OH	78	990	26.8	27	—	—
Methanol	CH_3OH	65	1214	19.9	16	—	—

* unknown; — not applicable; ≈ estimated value.

[a] From Refs. 7 and 12.

[b] $M = (CH_3)_3SiO_{1/2}$, $D = (CH_3)_2SiO$.

[c] $H_g = L + \int c_p \cdot dT$, where L is the heat of vaporization at T_b.

[d] Does not exhibit a characteristic boiling point.

[e] Approximate onset temperature for thermal degradation (reversion) to volatile cylics ($D_3, D_4, \ldots, D_n$); L ≈ 170–210 kJ/mole.

[f] MMA = methylmethacrylate

[g] H_c with gaseous water as a product.

tion product and there is no comparable loss mechanism. Ash breaks out of flames burning a silicon containing fluid for all mass fluxes.

Pool fires provide a convenient, controlled means for studying the burning behavior of a material. Fundamental fire parameters such as the mass flux (the mass burning rate per unit area of pool surface), the radiative and convective components of the heat release, and their dependence on fire size (scale effects) can be deduced from pool fires, for example see Refs. 8–11.

The objective of the present study was to quantify the radiative fraction of the heat release for silicone fluids as a function of burner diameter and fluid chain length. In order to accomplish this, the mass burning rate and the spatial distribution of radiative flux were measured in steady-state pool fires. A procedure was developed to account for silica ash deposition into the burning fluid. A wide range of silicone fluids was investigated and their global combustion behavior was compared to a number of organic compounds.

EXPERIMENTAL METHOD

The design of the pool and fuel control systems was based on that used by Hamins et al. [9]. All burners were 0.1 m in depth and ranged in diameter from 0.1 to 1 m. The fuel-feed system was gravity driven. A thermocouple was used as a fuel-level sensor, facilitating a constant fuel level in the burner. A load cell measured the mass of fuel in the reservoir as a function of time. The change in the measured mass indicated the mass burning flux. Reported measurements refer to times after a steady mass flux was achieved. This system provided excellent measurement and control of the supply of fluid to the burner for the larger pan burns (0.3 m and 0.6 m) for both the hydrocarbons and the silicone fluids.

Several design and procedural changes in the fuel-feed system were necessary because of fouling of the thermocouple located near the fuel surface by the silica for all 0.1-m pool burns (silicones) and 0.3-m pool burns of the $MD_{15}M$ and $MD_{58}M$ silicone fluids. A schematic of the modified apparatus is shown in Fig. 1. The key feature of this system is the use of a constant hydrostatic pressure head on the burette, which provided a steady supply of fuel to the "fuel-feed" reservoir (see Fig. 1). The mass flux of the fuel was equal to the difference in the measured rate of increase in the load cell mass taken prior to ignition (with the fuel feed valve shut off) and during steady-state burning. A constant fuel level in the pool was maintained throughout each burn and could be varied by adjusting the relative position of the "fuel-feed" reservoir. Fuel level (or lip height) in the burner can influence the mass flux. This was found to be most pronounced for the smallest diameter pools. A shallow lip height of 2–3 mm was used for low volatility fuels, whereas a lip height of 10–15 mm was necessary for the volatile fuels to eliminate the possibility of fuel flowing over the edge of the burner.

Two additional significant complications arise from the deposition of silica from the flame into the fluid. First, the fuel mass flux must be corrected for the displacement of fuel in the pool by silica, resulting in a somewhat larger mass flux than indicated by the load cell measurements:

$$\dot{m}_{corr} = \dot{m}_{unc} + (\dot{m}_{Sil}/\rho_{Sil})\rho_{F,T} \qquad (2)$$

where $\dot{m}_{corr}$ is the corrected mass flux, $\dot{m}_{unc}$ is the uncorrected or apparent mass flux, $\dot{m}_{Sil}$ is the deposition rate of silica into the fuel, $\rho_{F,T}$ is the density of the fluid at pool temperature, and ρ_{Sil} is the density of silica (2.2 g/cc). The deposition rate of silica was determined by assaying the fluid in the pool at the conclusion of the burn for silica content. The silica deposition rate was assumed to be constant throughout the burn. The average expanded uncertainty (2σ) in the silica deposition rate ($\dot{m}_{Sil}$) was 22%, based on measurement variance.

Second, the silica deposited on the surface of the fuel and the edge of the pool during the course of the burn results in a continual and erratic reduction of the mass flux. A silica layer is typically formed at the inner edge of the burner rim and grows radially in toward the pool center until the entire surface is covered by silica. These edge deposits of silica can also

result in fuel wicking (capillary effects) over the burner rim. Removal of the silica from the edge of the pool was accomplished by gentle, continuous scraping of the inner edge during the burn by means of a long-handled, narrow blade (7 mm) stainless steel spatula. Scraping the inner rim of the burner reduces silica accumulation at the surface of the liquid resulting in a constant mass flux, which is essential for the measurement of the radiative enthalpy loss fraction from the flame. This silica control procedure was necessary for all silicone burns in the 0.1-m pool and only the $MD_{15}M$ and $MD_{58}M$ fluid burns in the 0.3-m pool. In several instances, mass fluxes were verified by actual mechanical addition of fluids to the pools via periodic additions of fuel from hypodermic syringes during an extended burn and carefully verifying the liquid level in the pool. The average expanded uncertainty (2σ) in the corrected mass flux ($\dot{m}_{corr}$) was 10%, based on measurement variance.

Radiometers were calibrated using a tungsten lamp and a certified radiometer as primary reference standard. A mobile radiometer system consisting of two radiometers positioned on an electronically controlled X–Y translation apparatus was used for all 0.1-m pool burns and 0.3-m pool burns of $MD_{15}M$ and $MD_{58}M$ silicone fluids. The radiant flux was measured in the radial (14 points) and a vertical (18 points) planes for at least 30 s/location at a rate of 10 Hz. The measurements were time averaged. A fixed array of radiometers (6 = radial and 9 = vertical) was used for the 0.3- and 0.6-m pool burns. In all cases, appropriate corrections for background were made. These corrections were especially significant for fuels with low radiant emission (e.g., alcohols and long-chain silicone fluids). A double set of fine-wire mesh (4/cm) screens was placed around the pool fires to minimize disruption of the fire plume and to enhance cylindrical symmetry of the fire.

Flame ignition for the longer chain length silicone fluids could only be accomplished by prior heating of the fluid. For the longest chain length fluid ($MD_{58}M$) in the 30-cm pool, it was necessary to raise the fluid temperature to higher than 300°C to achieve ignition and sus-

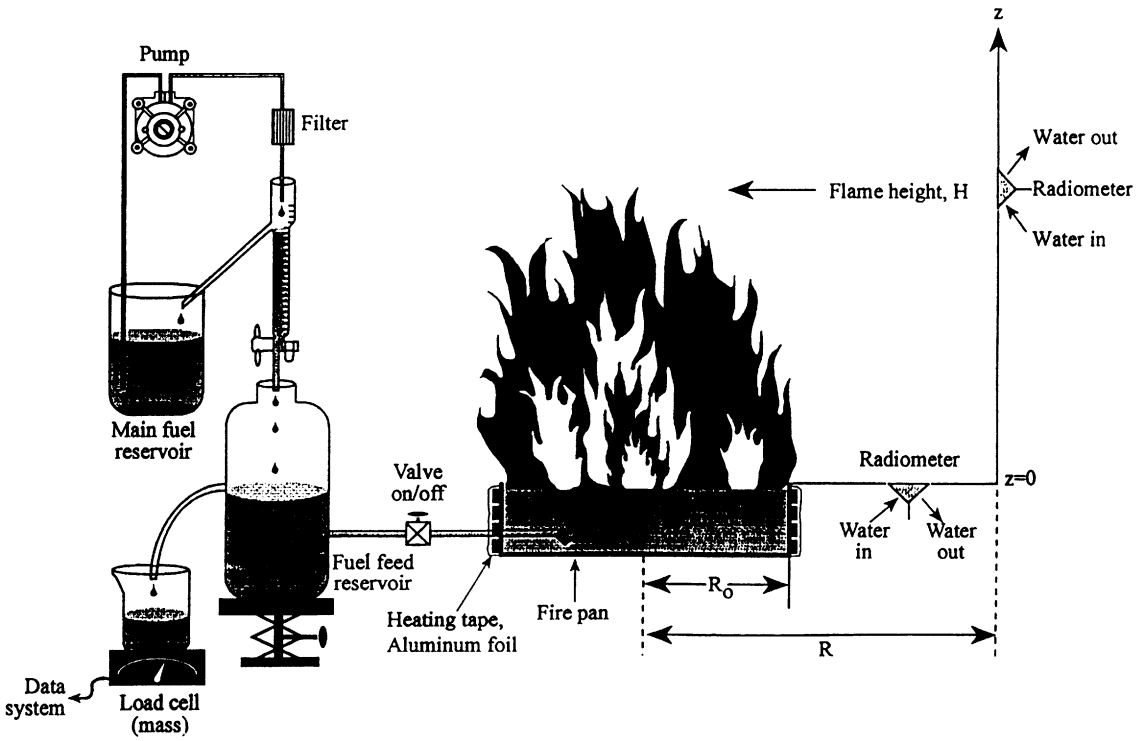

Fig. 1. Schematic diagram of the constant hydrostatic head fuel-supply system.

tained burning of the fluid. After ignition, heating of the pools was terminated. Preheating also facilitated rapid attainment of steady-state mass flux. Fuel temperature was monitored using a Type K thermocouple located approximately 0.01 m below the fuel surface near the center of the pool.

Radiative Enthalpy Losses

Radiative enthalpy measurements commenced 15 to 30 min after ignition of the fuel, that is, when a constant mass flux was observed. The steady-state radiative heat flux from the flame was measured at multiple locations on a cylindrical control surface surrounding the fire, similar to a previously described method [9]. Measurements were time-averaged at each location for a minimum of 30 s and typically 120 s for the mobile radiometer system. Data were collected for 15 to 30 min with the fixed radiometer system. The total radiated power ($\dot{Q}_r$) emitted by the flame, was determined by numerically integrating the measured vertical (z) and radial (r) distributions of radiative flux ($\dot{q}''$) using the following expression:

$$\dot{Q}_r = 2\pi \cdot \left(\int_{Ro}^{R} r \cdot \dot{q}''(r) \cdot dr + R \cdot \int_{0}^{\infty} \dot{q}''(z) \cdot dz \right) \quad (3)$$

where R represents the distance from the pool center to the vertical radiometer measurement axis (see Fig. 1). Typical measured radiative fluxes are shown in Figs. 5 and 6 for a range of fuels used in this study. The average expanded uncertainty (2σ) in $\dot{Q}_r$ was 19%, based on measurement variance. The total heat-release rate ($\dot{Q}$) is calculated from H_c and the fuel mass gasification rate or the corrected fuel mass gasification rate:

$$\dot{Q} = \dot{m} \cdot H_c \quad (4)$$

where H_c is the net heat of combustion (kJ/g) listed in Table 1. The measurement of $\dot{Q}_r$(W), in conjunction with the measurement of $\dot{m}$ allows determination of the radiative enthalpy loss fraction (χ_r), which is defined as:

$$\chi_r = \dot{Q}_r/\dot{Q} \quad (5)$$

The expanded uncertainty (2σ) in χ_r was calculated as 22% from a propagation of error analysis.

RESULTS AND DISCUSSION

Figure 2 shows the mass gasification rate corrected for silica deposition ($\dot{m}_{corr}$) as a function of the silicone chain length, n, for 0.10-m diameter pool fires. The lines in this and subsequent figures represent trends in the data. The silica deposition correction resulted in a significant correction to the apparent mass flux for the longer chain length fluids, in some cases as much as 15%. For the short-chain silicone oligomers, the silica deposition correction was less than 1% for 0.3-m diameter burners (and larger), whereas the correction was less than 5% in the 0.1-m burner. The silica deposition yield is defined as the ratio of the mass deposition rate of silica into the pool ($\dot{m}_{Sil}$) to the fluid mass gasification rate. The silica deposition yield increased with chain length as shown in Fig. 2. The inverse relationship between the mass gasification rate and the SiO_2 deposition yield suggests that the mass gasification rate and fire plume buoyancy regulate the amount of silica deposited into the pool. Consistent with this notion, the SiO_2 yield increased significantly with pool size, implying that the larger the fire, the lower the transport of ash into the plume. The ash collected in the pool was analyzed for carbon, silicon, and hydrogen content and was found to be predominantly ($\approx$ 90% by mass) silicon dioxide (silica).

The mass gasification rate of the longer chain silicones was much smaller, due in part to the very large heat of gasification and the small value of H_c/H_g (see Table 1). The net heat of combustion varies less than 30% for the silicone fluids (see Table 1) and H_c/H_g has been shown to approximately correlate the mass flux of large diameter hydrocarbon pool fires [10].

Figure 3 shows a comparison of the corrected mass flux for silicone fluids burning in 0.10- and 0.30-m diameter burners. Mass fluxes differ slightly for the longer chain silicones in the 0.10- and 0.30-m diameter pools but diverge substantially for the shorter chain

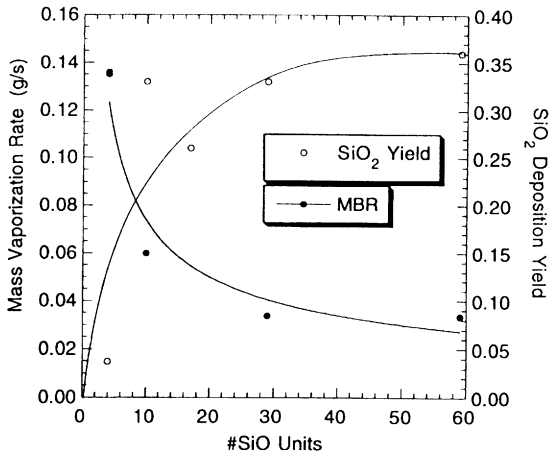

Fig. 2. The corrected mass gasification rate and silica deposition yield as a function of silicone chain length for 0.10-m diameter pool fires.

oligomers. This is not unlike the burning of organic compounds. The small primary alcohols, for example, methanol and ethanol, are characterized by mass fluxes that were nearly constant as a function of burner diameter over the range of diameters tested, whereas the mass flux of hydrocarbons increased with increasing pool diameter. These results on silicones compare favorably with earlier observations on their burning behavior using the cone calorimeter [4]. That is, oligomeric silicones exhibit a marked dependence on fire size, that is, pool size or applied external heat flux, whereas longer chain length silicones ($n > 15$) are quite insensitive to fire size. Similarly, the partitioning behavior (plume fraction versus surface deposited fraction) of silica in this study correlates well with the earlier cone-calorimeter study.

Figure 4 shows the corrected mass flux as a function of burner diameter for a number of silicone fluids. Our measurements of the mass flux for a number of organic fuels are also shown. As the burner diameter increased, the mass flux for the longer chain silicones was approximately constant, not unlike the results for methanol and ethanol. All these materials exhibit very low particulates in their fire plumes. The mass flux for the shorter chain silicone oligomers increased substantially with burner diameter, however, with a slope not unlike the hydrocarbons tested. Fires burning these silicone oligomers are highly luminous, suggesting high-energy feedback from the fire plume to the fluid surface. This in combination with the relatively low heats of gasification for the silicone oligomers results in high mass fluxes for these materials.

The measured near field time-averaged radiative heat flux as a function of location in the radial and vertical directions about the fire for

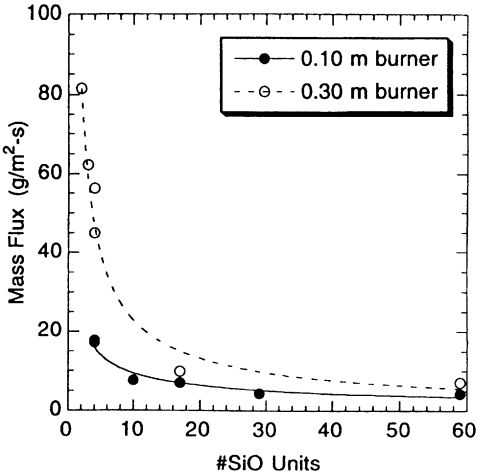

Fig. 3. The corrected mass flux as a function of silicone chain length for 0.10- and 0.30-m diameter pool fires.

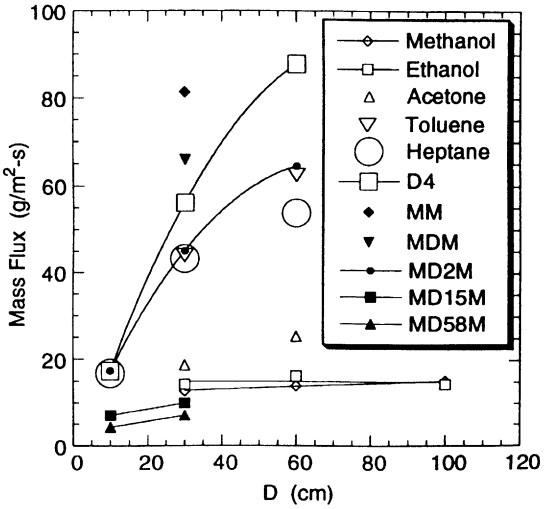

Fig. 4. The mass flux as a function of burner diameter for organic and silicone fluids.

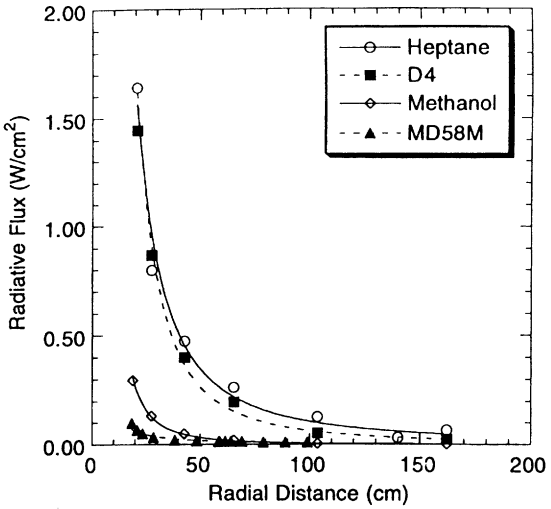

Fig. 5. The radiative heat flux as a function of location in the radial direction for 0.30-m diameter pools burning heptane, methanol, D_4, and $MD_{58}M$.

0.3-m diameter pools burning heptane, methanol, D_4, and $MD_{58}M$ are given in Figs. 5 and 6. Figure 5 shows that the flux drops off quickly in the radial direction away from the fire, whereas Fig. 6 shows that the flux obtains a maxima at some intermediate distance along the vertical axis. This is consistent with earlier findings [9]. The magnitude of the radiative heat flux for the heptane fire in both the radial and vertical directions is similar to the D_4 fire and much larger than the methanol or $MD_{58}M$ fluid, which also have similar heat flux profiles. The lower radiative fluxes are associated with the slower burning fuels and the relatively non-luminous fire plumes.

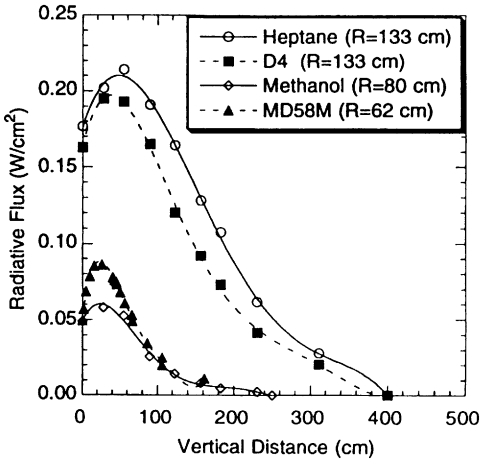

Fig. 6. The radiative heat flux as a function of location in the vertical direction for 0.30-m diameter pools burning heptane, methanol, D_4, and $MD_{58}M$. The value of R (see Fig. 1) is indicated for each experiment.

The time-averaged radiative power (calculated using Eq. 3 and the measured radiative flux profiles, such as shown in Figs. 5 and 6) for a number of organic and silicone fluids as a function of burner diameter is shown in Fig. 7. $\dot{Q}_r$ differs by approximately an order of magnitude between fuels, the difference increasing somewhat with pool diameter. The average radiative power ($\dot{Q}_r$) for the silicone oligomers (MM, MD_1M, MD_2M, and D_4) was similar to that of the hydrocarbons tested, whereas the less volatile, longer chain lengths silicones ($MD_{15}M$ and $MD_{58}M$) radiated substantially less, not unlike the alcohols (methanol and ethanol). The range of radiative power exhibited by the materials in this study posed several significant challenges.

Figure 8 shows χ_r for a number of organic and silicone fluids, the same fuels shown in Fig. 7. For the shorter chain length silicones and the hydrocarbons, χ_r increased from approximately 0.3 to 0.45 as the burner diameter increased from 0.1 to 0.6 m. For the longer chain length silicones and the alcohols, how-

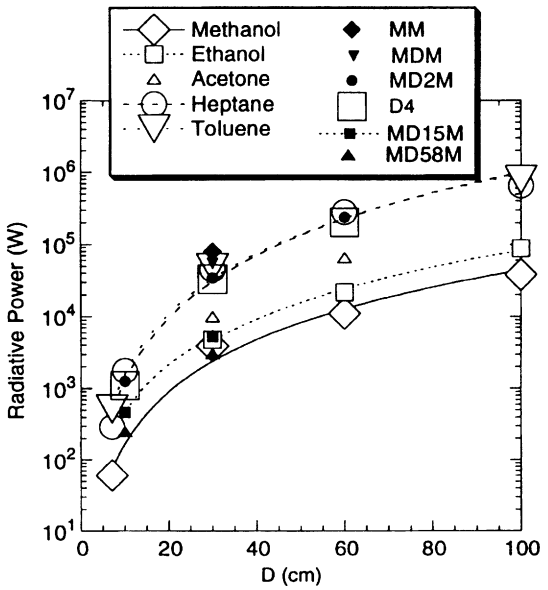

Fig. 7. The radiated power as a function of pool diameter for a number of organic and silicone fluids.

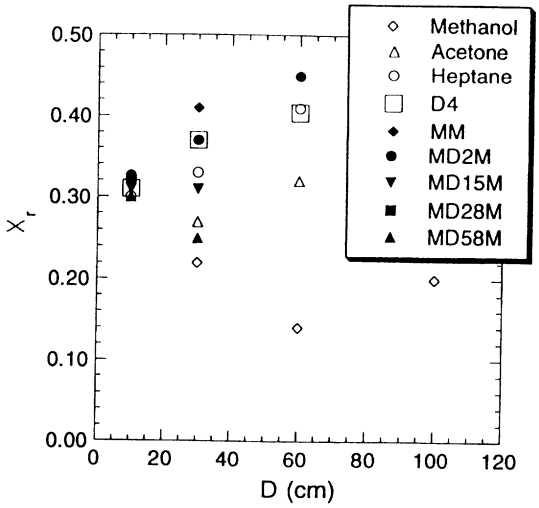

Fig. 8. The radiative heat loss fraction (χ_r) for a number of organic and silicone fluids.

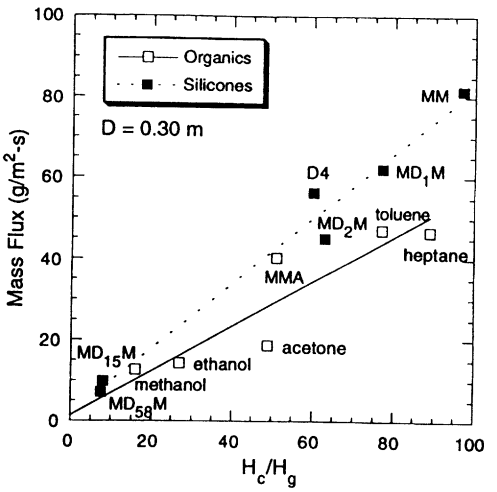

Fig. 9. The mass flux as a function of H_c/H_g for a number of organic and silicone fluids.

ever, χ_r remained nearly constant with burner diameter. The reduction in χ_r for the slower burning (longer chain length) fluids resulted perhaps from the markedly reduced amount of particulates in the fire plumes. Virtually all of the silica particulates formed during combustion of the shorter chain (and most volatile) fluids are removed via convective transport through the plume, whereas the silica deposition yield into the pool (Eq. 6) is $\approx$ 50% for the longer chain length fluids. As shown in Fig. 2, the silica yields correlated inversely with the mass gasification rate, indicating that the fate of the particulates (falling into the pool or convected away from the fire) is related to the magnitude of the plume buoyancy forces, which are associated with fire heat-release rates.

Figure 9 shows the measured mass flux as a function of H_c/H_g for a number of organic fuels and silicone fluids. Burgess and Hertzburg [10] suggested that such a plot correlates the mass flux for hydrocarbons in the limit of large burner diameters. Large diameter data are not available for the silicones, thus only the 0.30-m pool diameter results are shown in Fig. 9. As H_c/H_g increased, the mass flux increased for both the organic fuels and the silicone fluids. H_c/H_g appears to adequately correlate the mass fluxes for both the organics and the silicone fluids.

Figure 10 shows that χ_r is also independently correlated by H_c/H_g for the organics and the silicone fluids. In general, χ_r was larger for the silicone fluids (oligomers) as compared to the organic fuels. In addition, the longer chain length silicone fluids radiated far less than the short-chain silicones. We speculate that this may be due to a smaller silica ash volume fraction in the flames burning the long-chain silicones where a large fraction of the silica falls back onto the liquid fuel (see Fig. 2). Differences in χ_r for the organic fuels as compared to the silicone fluids are likely caused by differences in flame structure (i.e., the spatial distribution of particle volume frac-

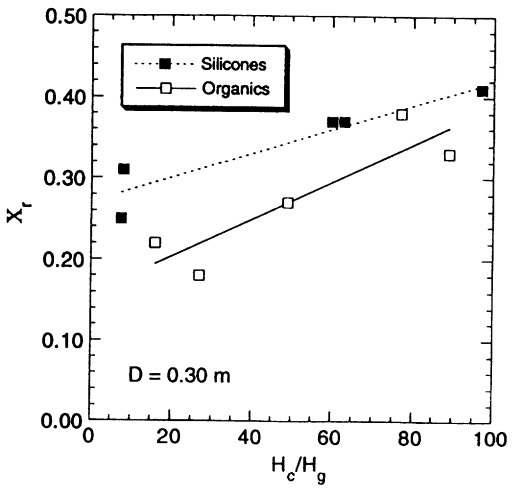

Fig. 10. The radiative heat loss fraction (χ_r) as a function of H_c/H_g for a number of organic and silicone fluids.

tion, the size distribution of the particles, the radiative characteristics of the silica ash as compared to carbonaceous soot particles, the spatial temperature distribution, and so on). Detailed flame measurements of the distribution of flame temperature and ash volume fraction may clarify this issue. In any case, a larger radiative fraction in fires burning silicone fluids as shown in Fig. 10 could contribute to larger radiative heat feedback to the fuel surface for these fluids as compared to the organics, representing a possible mechanism for the higher mass fluxes shown in Fig. 9 for the silicone fluids.

SUMMARY AND CONCLUSIONS

The mass flux and the radiative fraction of the heat release were measured as a function of burner diameter and silicone fluid chain length in steady-state pool fires. The fire parameters varied markedly with chain length of the silicone fluid. Short-chain silicone oligomers and aliphatic/aromatic hydrocarbons exhibited a strong dependence of the mass flux and the radiative fraction on pool size.

The longer chain length silicone fluids and alcohols exhibited both markedly lower mass fluxes and lower radiative components of heat release and these parameters were virtually independent of pool size. The mass flux and the radiative heat loss fractions were found to independently correlate with H_c/H_g for the organic fuels and the silicone fluids.

Silica ash was observed to form in the gas phase. Typically, agglomerates of ash fell back to the surface of the liquid pool where they collected and subsequently submerged. The apparent mass flux was corrected accordingly, based on assays of the ash in the unburnt fuel at the conclusion of the experiment. Partitioning of the silica to either the fuel surface or fire plume is largely dictated by convective transfer generated by the fire, which is related to the fuel mass flux and the fire heat-release rate. The rate of ash deposition on the fuel surface was largest for the slower burning longer chain length fluids. The collected ash was analyzed for carbon, silicon, and hydrogen content and found to be almost exclusively amorphous silicon dioxide. The effect of porosity and depth of the silica layer covering the pool surface and its influence on burning behavior is currently under investigation.

REFERENCES

1. Hemstreet, R. A., *Flammability Tests of Askarel Replacement Transformer Fluids*. Factory Mutual Research Corp. FMRC Serial No. 1A7R3, RC, 1978.
2. Kanakia, M., *Characterization of Transformer Fluid Pool Fires by Heat Release Rate Calorimetry*, Presented at the 4th International Conference on Fire Safety, University of San Francisco, 1979.
3. Tewarson, A., *Fire Behavior of Transformer Dielectric Insulating Fluids*, Report #FRA/ORD-80/08, Prepared for Dept. of Transportation, January 1980.
4. Buch, R. R., *Fire Safety J.* 17:1 (1991).
5. Lipowitz, J., *J. Fire Flam.* 7:482 (1976).
6. Lipowitz, J., and Ziemelis, M. J., *J. Fire Flam.* 7:504 (1976).
7. Flaningam, O. L., and Langley, N. R., in *Physical Properties and Polymer Structure* (A. L. Smith, Ed.), Wiley, New York, 1991, Chapter 7.
8. Spalding, D. B., *Some Fundamentals of Combustion*, Butterworths, London, 1955.
9. Hamins, A., Kashiwagi, T., Gore, J., and Klassen, M., *Combust. Flame* 86:223 (1991).
10. Burgess, D., and Hertzburg, M., in *Heat Transfer in Flames* (N. H. Afgan and J. M. Beers, Eds.), Wiley, New York, 1974, Chapter 27.
11. Blinov, V. I., and Khudiakov, G. N., (Institute of Energetics of the Academy of Sciences, USSR), *Academia Nauk, SSSR Doklady* 113:1094 (1957).
12. Daubert, T. E., and Danner, R. P., *Physical and Thermodynamic Properties of Pure Chemicals (Design Institute for Physical Property Research, DIPPR, Data Compilation)*, Taylor & Francis, Bristol, PA, 1995.

Received 13 November 1995; accepted 12 April 1996.